Laboratory Investigation

Early Hemodynamic and Biochemical Changes in Overloaded Swine Ventricle

Sandro Gelsomino, MD, PhD
Fabiana Lucà, MD
Chiara Nediani, MD
Sandra Zecchi Orlandini, MD
Daniele Bani, MD
Antonio S. Rubino, MD
Attilio Renzulli, MD, PhD
Roberto Lorusso, MD, PhD
Andrea Consolo, MD
Antonino Lo Cascio, MD
Jos Maessen, MD, PhD
Gian Franco Gensini, MD

Key words: *Aortic valve stenosis/pathology; calcium; calcium-transporting ATPases; disease models, animal; hemodynamics; myocardial contraction/physiology; sarcoplasmic reticulum/physiology; sarcoplasmic reticulum calcium-transporting ATPases; swine*

From: *Experimental Surgery Unit, Heart and Vessels Department (Drs. Gelsomino, Gensini, Lorusso, and Lucà), Careggi Hospital, 50134 Florence, Italy; Departments of Biochemical Sciences (Dr. Nediani) and Human Anatomy and Histology (Drs. Bani and Zecchi Orlandini), University of Florence, 50134 Florence, Italy; Cardiac Surgery Unit (Drs. Renzulli and Rubino), University of Magna Graecia, 88100 Catanzaro, Italy; Cardiology Unit (Drs. Consolo and Lo Cascio), Barone Romeo Hospital, Patti, 98066 Messina, Italy; and Department of Cardiothoracic Surgery (Drs. Gelsomino, Lucà, and Maessen), Academic Hospital Maastricht, 6229 HX Maastricht, The Netherlands*

Address for reprints: *Sandro Gelsomino, MD, PhD, Heart and Vessels Department, Careggi Hospital, Via delle Oblate 1, 55100 Florence, Italy*

E-mail: *sandro.gelsomino@libero.it*

The present study was undertaken to investigate, in an animal model, the relationship between sarcoplasmic reticulum Ca^{2+}-ATPase (SERCA2a) activity, phospholamban phosphorylation, acylphosphatase activity, and hemodynamic changes that occur in the early phase of pressure overload.

In 54 study-group pigs, weighing 40 ± 5 kg each, an aortic stenosis was created with a band of umbilical tape tied around the aorta; 18 sham-operated pigs formed our control group. Eight animals (6 study and 2 control) were randomly assigned to each experimental time (0.5, 3, 6, 12, 24, 48, 72, 96, and 168 hr).

All indices of left ventricular function declined significantly, with a peak at 6 hr and a return to baseline at 168 hr. At each observational time, SERCA2a activity, Ca^{2+} uptake, and acylphosphatase activity rose significantly, with a maximum increase at 6 hr. These changes indicated a higher expression of these proteins; conversely, phospholamban did not show significant changes in its concentration or in its phosphorylation status. Nuclear proto-oncogene c-fos expression rose at 6 hr. A strong inverse correlation was found when Ca^{2+}-ATPase activity, Ca^{2+}-ATPase expression, Ca^{2+} uptake, and acylphosphatase were compared with indices of systolic function.

In our model of induced pressure overload, an initial phase of depressed myocardial contractility was accompanied by an increased sarcoplasmic reticulum function and by higher Ca^{2+}-ATPase and Ca^{2+} uptake activities mediated by acylphosphatase. This new finding of Ca^{2+} homeostasis might indicate a compensatory mechanism for mechanical stress. Further studies are needed to confirm our findings. ***(Tex Heart Inst J 2013;40(3):235-45)***

In the presence of pressure overload, left ventricular hypertrophy (LVH) is an adaptive mechanism that normalizes parietal wall stress and contributes to the preservation of normal left ventricular (LV) function.[1,2] Myocyte Ca^{2+} handling plays a pivotal role in cardiac excitation-contraction coupling,[3] and hypertrophy is associated with changes in sarcoplasmic reticulum (SR) and sarcoplasmic reticulum Ca^{2+}-ATPase (SERCA2a) function.[4]

However, changes in SR function have also been observed during the acute phase of pressure overload, when the hypertrophy has not yet fully developed; this results in enhanced SR function with increased levels of acylphosphatase, a cytosolic enzyme well represented in cardiac muscle, which might contribute to this effect.[5] Furthermore, SERCA2a is regulated by phospholamban (PLB), a membrane protein whose cAMP-dependent phosphorylation leads to an enhancement of Ca^{2+} active transport.

The present study was undertaken to investigate, in an animal model, the relationship between SERCA2a activity, PLB phosphorylation, acylphosphatase activity, and hemodynamic changes that occur in the early phase of pressure overload.

Materials and Methods

The study was approved by our institutional ethics committee, and the animals were managed in accordance with the principles of the "Guide for the Care and Use of Laboratory Animals," Italian national law (DL. 116/1992), and the recommendations of the European Community (86/609/CEE) for the care and use of laboratory animals. All the experiments were carried out at the Experimental Cardiac Surgery Unit, Heart and Vessels Department, Careggi Hospital, Florence, Italy.

Seventy-two farm pigs, each weighing 40 ± 5 kg, were randomly assigned to 9 groups that corresponded to the experimental observational times (0.5, 3, 6, 12, 24, 48, 72, 96, and 168 hr), with a ratio of 3:1 between the 54 study-group animals and

the 18 sham-operated (control-group) animals. Therefore, 6 study and 2 control pigs were assigned to each experimental time.

All animals underwent preoperative intramuscular administration of 15 mg/kg ketamine and 5 mg/kg diazepam. General anesthesia was induced with intravenous administration of ketamine (3.5 mg/kg) and atropine sulfate 0.05 mg/kg. The trachea was intubated during spontaneous breathing, and the muscles were relaxed with 0.1 mg/kg pancuromium bromide. The lungs were ventilated in a volume-controlled mode with 40% oxygen at 16 to 20 breaths/min, and tidal volume was adjusted at 8 to 10 mL/kg to maintain partial carbon dioxide pressure ranging from 35 to 40 mmHg. Anesthesia was maintained with sevoflurane (2%–3%). The electrocardiogram was continuously monitored in a standard lead II, and oxygen saturation was monitored by a continuous pulse oximeter placed on the ear.

A Swan-Ganz catheter was introduced into the pulmonary artery through the right jugular vein to obtain pulmonary artery pressure, pulmonary capillary wedge pressure, and cardiac output, as determined by the thermodilution technique. A transesophageal probe was positioned and connected to the Vivid™ echocardiographic machine (General Electric Medical Systems; Milwaukee, Wisc). An aortic long-axis view was obtained, and the probe was fixed by maintaining an angle of 0° to 20° between the aortic blood flow and the continuous-wave Doppler beam.

A median sternotomy was performed, and the pericardium was opened longitudinally. An 18G catheter was introduced into the LV through the left atrial appendage to measure LV pressure. Aortic stenosis was created by tying a band of umbilical tape around the aorta to create a transvalvular gradient of 50 to 55 mmHg. The sternotomy was then closed. All subjects underwent postoperative treatment with penicillin (1,000,000 U/d) and an intramuscular analgesic agent (diclofenac, 75 mg). Pigs in the control group underwent the same surgical procedure without the creation of aortic stenosis.

Echocardiographic Data

All animals underwent echocardiography preoperatively, after surgery, and at all observational times. Measurements were first made in accordance with the recommendation of the American Society of Echocardiography.[6] Left ventricular mass was calculated in accordance with the Penn convention.[7] Relative wall thickness was the ratio of 2*WT/LVID, where WT is the end-diastolic wall thickness and LVID is the LV internal dimension.[8] Fractional shortening at the endocardium was calculated as the difference between the end-diastolic and end-systolic circumferences divided by the end-diastolic circumference and multiplied by 100.[8] Mid-wall fractional shortening (FS_{mw}) was calculated using a 2-shell cylindrical model.[9] Left ventricular volume and ejection fraction were obtained at end-diastole and end-systole by the modified Simpson's rule method.[10] Circumferential peak systolic (PSS_c), end-systolic (ESS_c), and end-diastolic (EDS_c) wall stresses were also estimated at midwall using a cylindrical model previously applied to clinical studies.[11] Meridional stresses were obtained by invasive LV pressure, using a validated formula.[12] Relations of FS_{mw} to circumferential end-systolic stress were examined and plotted with predicted values calculated from equations derived from controls. Examinations and measurements were carried out by one experienced echocardiographer (F.L.) The reliability of echocardiographic measurements was evaluated by calculating intraobserver intervals of agreement of main direct measures used in this study (end-diastolic diameter [EDD] and WT) in 20 pigs chosen at random. The Bland-Altman method showed excellent agreement between intraobserver measurements of echocardiographic parameters (EDD, bias 0.018 ± 0.003 [P <0.001]; WT, bias 0.002 ± 0.003 [P <0.001]).

Biochemical and Morphologic Evaluation

Biochemical and morphologic evaluations were performed as previously reported.[5] The Appendix sets forth the results in detail.

Statistical Analysis

Randomization was carried out by Stats Direct for Windows release 2.3.8 (Stats Direct Ltd.; Cheshire, UK), using the Mersenne twister algorithm of Matsumoto and Nishimura, which has a resolution of 32 bits and a period of $2^{19,937}$. The allocation sequence was generated by R.L. and A.S.R., who blindly assigned animals to the groups.

The power analysis was determined by GraphPad StatMate software, release 2.00 (GraphPad Prism Software, Inc.; San Diego, Calif) on the basis of the following assumptions: a type I error of 0.05 (2-sided) and a difference in EDD of 0.3 mm. The calculated statistical power was 0.90. Continuous data were expressed as mean ± SD. Data were compared for statistical significance using t tests, and multiple comparisons were carried out by analysis of variance with the Dunn post hoc test. The Pearson correlation was used to study univariate relations between variables. Biochemical–hemodynamic correlations were explored when an evident state of myocardial dysfunction occurred. Linear regression was applied to study the relationship between FS_{mw} and end-systolic circumferential wall stress. Log-transformation of circumferential wall stress was used in the regression, with midwall shortening as the best-fitting relation (R=0.9546, F=185.090, P <0.001). Significance was assumed when the P value was <0.05. For these calculations, we used SPSS 12.0 (IBM Corporation; Armonk, NY).

TABLE I. Echocardiographic Results

Variable	Controls	Baseline	0.5 hr	3 hr	6 hr	12 hr	24 hr	48 hr	72 hr	96 hr	168 hr
HR, beats/min	85 ± 8	87 ± 5	89 ± 7	110 ± 8*†	120 ± 4*†	102 ± 6*†	89 ± 8	90 ± 7	96 ± 8	92 ± 5	88 ± 5
ABP_s, mmHg	120 ± 8	111 ± 9	108 ± 10	113 ± 7	120 ± 5	118 ± 4	121 ± 4	120 ± 7	120 ± 5	119 ± 4	120 ± 6
ABP_d, mmHg	60 ± 8	66 ± 6	62 ± 5	73 ± 7	70 ± 9	66 ± 4	74 ± 4	68 ± 7	70 ± 8	68 ± 6	69 ± 4
Δp_s	9 ± 3	7 ± 2	47 ± 7*†	55 ± 4*†	55 ± 4*†	56 ± 5*†	57 ± 5*†	54 ± 4*†	54 ± 5*†	54 ± 5*†	56 ± 5*†
RVP_m, mmHg	25 ± 5	22 ± 3	27 ± 5	42 ± 9*†	50 ± 7*†	52 ± 8*†	50 ± 4*†	42 ± 6*†	38 ± 6*†	35 ± 7*†	32 ± 5*†
PWP_m, mmHg	11 ± 5	13 ± 4	14 ± 4	20 ± 2*†	25 ± 5*†	27 ± 3*†	23 ± 4*†	21 ± 5*†	20 ± 5*†	18 ± 4*†	16 ± 7*†
PSP, mmHg	167 ± 7	170 ± 5	171 ± 7	180 ± 9*†	198 ± 5*†	194 ± 5*†	190 ± 5*†	189 ± 3*†	190 ± 3*†	187 ± 3*†	180 ± 4*†
LVEDP, mmHg	11 ± 2	10 ± 2	10 ± 2	18 ± 2*†	19 ± 2*†	12 ± 2	12 ± 1	12 ± 1	11 ± 1	11 ± 1	11 ± 1
LVESD, mm	25 ± 4	27 ± 3	34 ± 3*†	28 ± 3	27 ± 2	25 ± 2	23 ± 1	23 ± 2	24 ± 2	23 ± 2	24 ± 1
LVEDD, mm	36 ± 4	35 ± 3	42 ± 3*†	43 ± 2*†	40 ± 3*†	35 ± 3	36 ± 2	36 ± 2	35 ± 2	36 ± 3	36 ± 3
WT_s, mm	11.4 ± 0.6	10.5 ± 0.4	9.7 ± 0.4*†	9.5 ± 0.9*†	10 ± 0.3	10.1 ± 0.3	10.1 ± 0.5	11.6 ± 0.3*†	11.4 ± 0.4*†	11.6 ± 0.3*†	11.5 ± 0.3*†
ST_s, mm	11.4 ± 0.4	11 ± 0.5	10.4 ± 0.3*†	10.6 ± 0.2*†	11.3 ± 0.2	10.8 ± 0.3	10.3 ± 0.3	12.2 ± 0.4*†	12 ± 0.4*†	12 ± 0.3*†	11.9 ± 0.3*†
RWT, mm	0.42 ± 0.03	0.44 ± 0.06	0.38 ± 0.04*†	0.39 ± 0.06*†	0.42 ± 0.04	0.45 ± 0.04	0.44 ± 0.04	0.5 ± 0.05*†	0.53 ± 0.06*†	0.55 ± 0.03*†	0.55 ± 0.03*†
LVM, g	84 ± 7	85 ± 9	75 ± 6*†	74 ± 11	80 ± 7	82 ± 8	83 ± 9	97 ± 9*†	98 ± 9*†	100 ± 14*†	102 ± 12*†
LVEF	0.65 ± 0.03	0.65 ± 0.07	0.63 ± 0.06	0.49 ± 0.12†	0.46 ± 0.08*†	0.56 ± 0.05*†	0.56 ± 0.06*†	0.56 ± 0.06*†	0.54 ± 0.06*†	0.59 ± 0.07*†	0.66 ± 0.07
FS_{endo}, %	36 ± 1.1	38 ± 1.2	34 ± 1.2	24 ± 1.1*†	22 ± 1.7*†	28 ± 1.3*†	30 ± 1.5*†	32 ± 1*†	34 ± 1.8	36 ± 1.9	38 ± 1.8
FS_{mw}, %	16 ± 1.1	17 ± 1.1	15 ± 1.1*†	15 ± 0.9*†	11 ± 1.1*†	12 ± 1*†	15 ± 1*††	15 ± 1.3*†	16 ± 1.2	16 ± 1.2	17 ± 1
CO, L/min	3,630 ± 475	3,500 ± 488	3,329 ± 463	3,143 ± 544*†	2,862 ± 490*†	2,912 ± 48*†	3,232 ± 488*†	3,208 ± 501*†	3,144 ± 434*†	3,341 ± 207	3,400 ± 221
CI, L/min/m^2	2 ± 0.5	1.9 ± 0.5	1.8 ± 0.4	1.7 ± 0.5	1.5 ± 0.3*†	1.6 ± 0.3*†	1.6 ± 0.3*†	1.6 ± 0.3*†	1.6 ± 0.4	1.6 ± 0.5	1.8 ± 0.5
SV, mL	44 ± 5	41 ± 4	39 ± 6	28 ± 5*†	23 ± 3*†	28 ± 3*†	36 ± 7*†	36 ± 3*†	36 ± 3*†	36 ± 4*†	39 ± 6

ABP_d = diastolic arterial blood pressure; ABP_s = systolic arterial blood pressure; CI = cardiac index; CO = cardiac output; Δp_s = systolic transaortic gradient; FS_{endo} = endocardial fractional shortening; FS_{mw} = mid-wall fractional shortening; HR = heart rate; LVEDD = left ventricular end-diastolic diameter; LVEDP = left ventricular end-diastolic pressure; LVEF = left ventricular ejection fraction; LVESD = left ventricular end-systolic diameter; LVM = left ventricular mass; PSP = left ventricular peak systolic pressure; PWP_m = mean pulmonary wedge pressure; RVP_m = mean right ventricular pressure; RWT = end-diastolic relative wall thickness; ST_s = left ventricular systolic septal thickness; SV = stroke volume; WT_s = left ventricular systolic posterior wall thickness

*P <0.05 versus baseline
†P <0.05 versus controls

P <0.05 was considered statistically significant.

Results

Hemodynamics

No animal died or had signs of cardiac failure during the observation period. Hemodynamic data are shown in Table I. At baseline, values were comparable in the study and control groups. Left ventricular end-diastolic (EDD) and end-systolic (ESD) diameters rose immediately after surgery and returned to baseline values at 3 and 12 hours, respectively. The LV peak systolic pressure exhibited significant increases at 3 and 6 hr ($P=0.001$ and $P<0.001$, respectively), which were maintained throughout the entire experimental period. The LV end-diastolic pressure significantly rose at 6 hr ($P=0.024$) and then gradually declined. Systolic wall thickness (WT_s), systolic septal (ST_s) thickness, LV mass, and relative wall thickness were reduced up to 6 hr ($P<0.001$ at all times) and then gradually increased, reaching statistical significance versus baseline at 48 hr (LV mass, $P=0.031$) and 72 hr ($P=0.03$ and $P=0.026$ for WT_s and ST_s , respectively) and remaining higher than baseline at 168 hr. All indices of LV function declined significantly from baseline and control-group values, with the maximum decline at 6 hr. All values returned to baseline within 168 hr.

Pulmonary artery pressures and pulmonary vascular resistances of the study group were comparable at baseline with those of the control group (Fig. 1). Both increased, reaching statistical significance at 168 hr.

Systolic and peak meridional stress rose immediately after surgery ($P=0.002$ vs baseline), peaked at 6 hr ($P<0.001$ vs baseline), and returned to baseline at 96 hr ($P=0.35$) and 48 hr ($P=0.6$), respectively. In contrast, end-diastolic stress (EDS_m) rose more sharply, remaining higher at 3 hr ($P=0.01$ vs baseline) and 6 hr ($P<0.001$ vs baseline) and reaching baseline values at 24 hr ($P=0.9$). Meridional stress values of the study group remained significantly higher than those of the control group for up to 48 hr (Fig. 2A). Circumferential wall stresses were elevated immediately after banding. Although ESS_c returned to base value at 12 hr, PSS_c and EDS_c did not normalize until 24 hr had passed (Fig. 2B).

The relationships of FS_{mw} to ESS_c are shown in Figure 3. At 3 hr, 17% of the animals were below the 95% normal confidence interval (CI). At 6 hr, this percentage was 88% ($P<0.001$), which confirmed a significant reduction in myocardial function at that observational time. At 168 hr, recovery was complete.

Biochemistry

As shown in Figures 4A and 4B, both Ca^{2+}-ATPase activity and Ca^{2+} uptake were significantly enhanced in the hearts of pressure-overloaded pigs, compared with the sham-operated animals. Although these values were higher than those of the control group after the onset of pressure overload (all $P<0.001$), the maximum increases (1.92-fold and 2.1-fold for the control values for Ca^{2+}-ATPase activity and Ca^{2+} uptake, respectively) were observed at 6 hr. Figure 4C shows the acylphosphatase activity assayed in the LVs of control-group and pressure-overloaded hearts. At 6 hr, the acylphosphatase activity was 2.5-fold higher in the pressure-overloaded hearts, reaching its highest increase. In the following stages, the level of acylphosphatase activity gradually decreased, following a trend very similar to that observed for functional changes in Ca^{2+} pumping.

To evaluate whether the alteration in the activity of the Ca^{2+} pump might be due to modifications in SERCA2a mass concentration or in PLB levels, we used an immunoblotting technique to evaluate the expression of these proteins. Figure 5 shows results of Western blot analysis of SERCA2a (Fig. 5A), PLB (Fig. 5B), and acylphosphatase (Fig. 5C), from study-group and control-group pig hearts. SERCA2a was significantly higher in

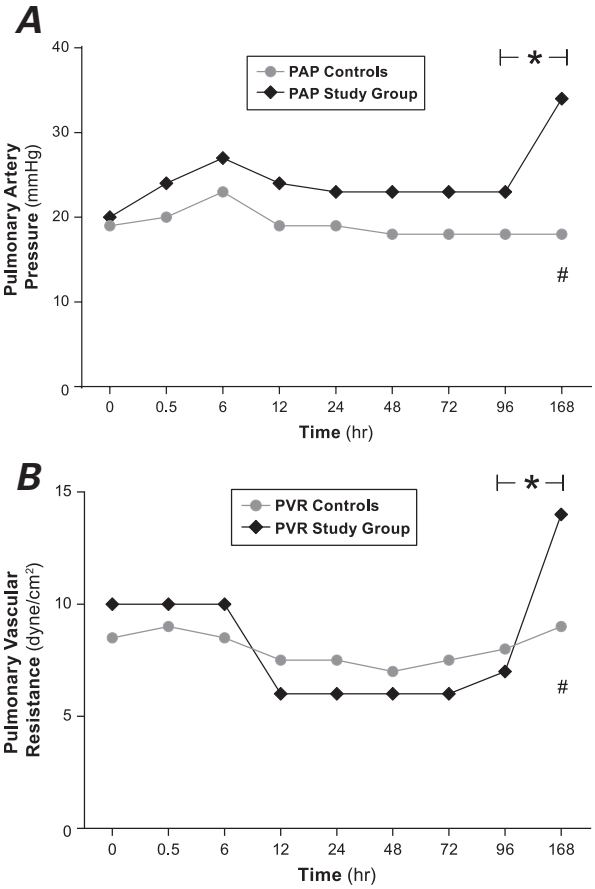

Fig. 1 ***A****) Pulmonary artery pressure (PAP) after banding and in the control group. The PAP increased slightly, early after banding, but it rose significantly at 168 hr (*P*=0.001 vs baseline; P <0.001 vs control group).* ***B****) Pulmonary vascular resistance (PVR) after banding and in the control group. The PVR dropped slightly after 12 hr (*P*=0.06) and increased significantly at 168 hr (*P*=0.026 vs baseline; P <0.001 vs control group).*

**Significance versus baseline*
#Significance versus control group

the study group, reaching its maximum expression at 6 hr (P <0.001). In contrast, PLB did not show any difference in expression between control and study groups. Our high-resolution procedure enabled us to take into consideration the changes in electrophoretic mobility resulting from PLB phosphorylation.[13] This finding—reinforced by densitometric analysis—suggests the absence of significant differences in PLB expression and PLB phosphorylation status between study-group and control-group hearts. Acylphosphatase protein levels showed a trend that paralleled changes in the activity of the Ca^{2+} pump.

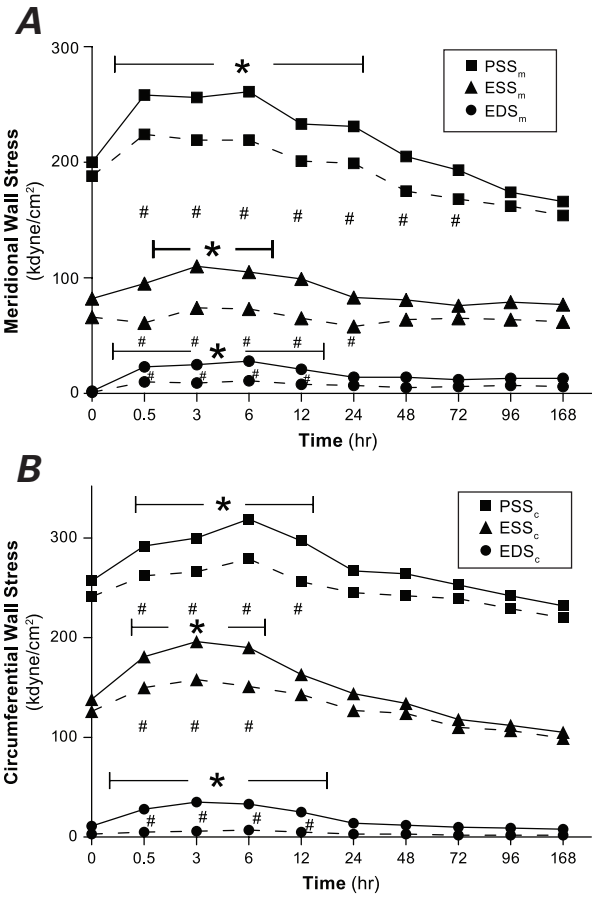

Fig. 2 ***A****) Meridional wall stress in overloaded swine ventricle. Peak-(PSS_m) and end-systolic (ESS_m) stresses increased immediately after surgery (both* P *<0.001 vs baseline) and peaked at 6 hr (both* P *<0.001 vs baseline), returning to baseline at 96 hr (*P*=0.8) and 48 hr (*P*=0.8), respectively. End-diastolic stress (EDS_m) rose more sharply (*P*=0.03 vs baseline) and returned to baseline at 24 hr (*P*=0.9).* ***B****) Circumferential wall stress in overloaded swine ventricle. Peak (PSS_c), end-systolic (ESS_c), and end-diastolic (EDS_c) values rose immediately after banding (*P*=0.01 and* P*=0.04, respectively). Although ESS_c returned to basal value at 12 hr (*P *>0.9), PSS_c and EDS_c normalized after 24 hr (*P*=0.8 and* P*=0.9, respectively).*

Continuous line: study group; dotted line: control group

**Significance versus baseline*
#Significance versus control group

Morphology

Immunofluorescence analysis with the aid of antibody anti-c-fos revealed, among cardiomyocytes, a significant increment in nuclear proto-oncogene c-fos expression, which occurred at 6 hr (Fig. 6). No nuclear reactivity was detected at the following observations. Transmission electron microscopic examination showed some derangement, with rarefaction of contractile myofilaments, loss of sarcomers, and intermyofibrillar edema occurring at 6 hr and not observed in control-group hearts. These alterations were focal, so normal cells lay

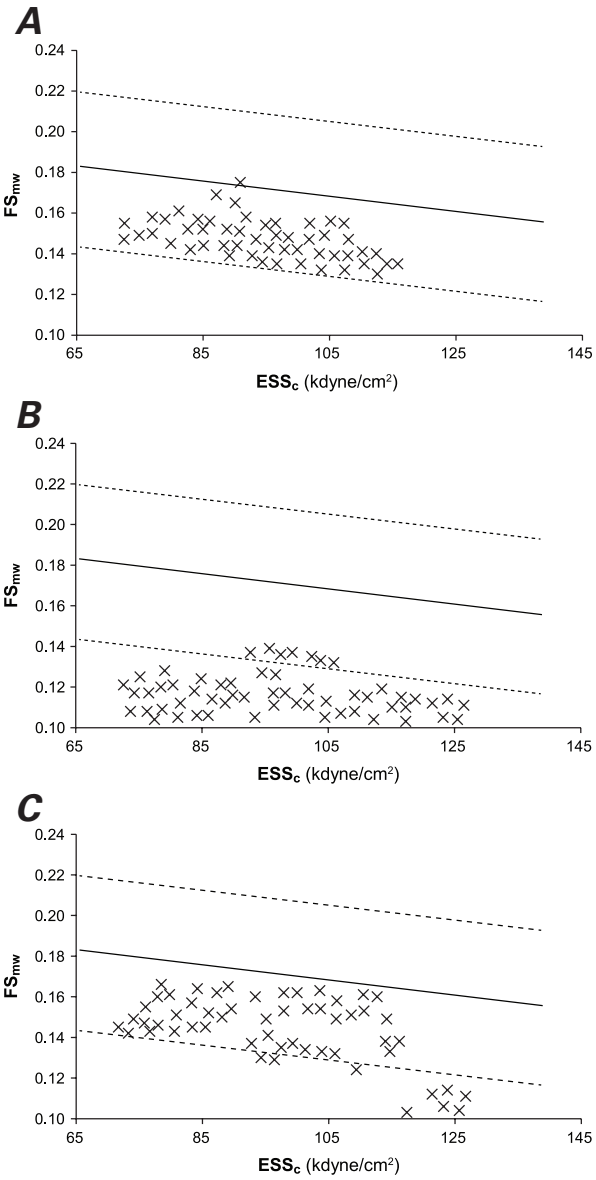

Fig. 3 *Relationships of midwall fractional shortening (FS_{mw}) with end-systolic circumferential wall stress (ESS_c) at different observational times. Regression line (solid line) and 95% confidence interval (CI) (dashed line).* ***A****) At baseline, all animals fell within 95% normal CI.* ***B****) At 6 hr from banding, 88% were below 95% CI.* ***C****) At 72 hr, FS_{mw} recovered but 38% of pigs still fell below 95% of predicted values.*

close to areas of damaged myocytes. The nuclei, mitochondria, cisternae of sarcoplasmic reticulum, and T tubules were rather normal. It is of interest that derangements declined after 12 hr and disappeared after 96 hr. Nonetheless, at that time (96 hr), clear ultrastructural signs of tissue damage appeared, such as intracellular and extracellular edema, swollen mitochondria, fragmentation of mitochondrial cristae, and dissolved mitochondrial matrix. Furthermore, activated fibroblasts were observed in the interstitial space, revealing many cisternae of rough endoplasmic reticulum and a well-developed Golgi apparatus.

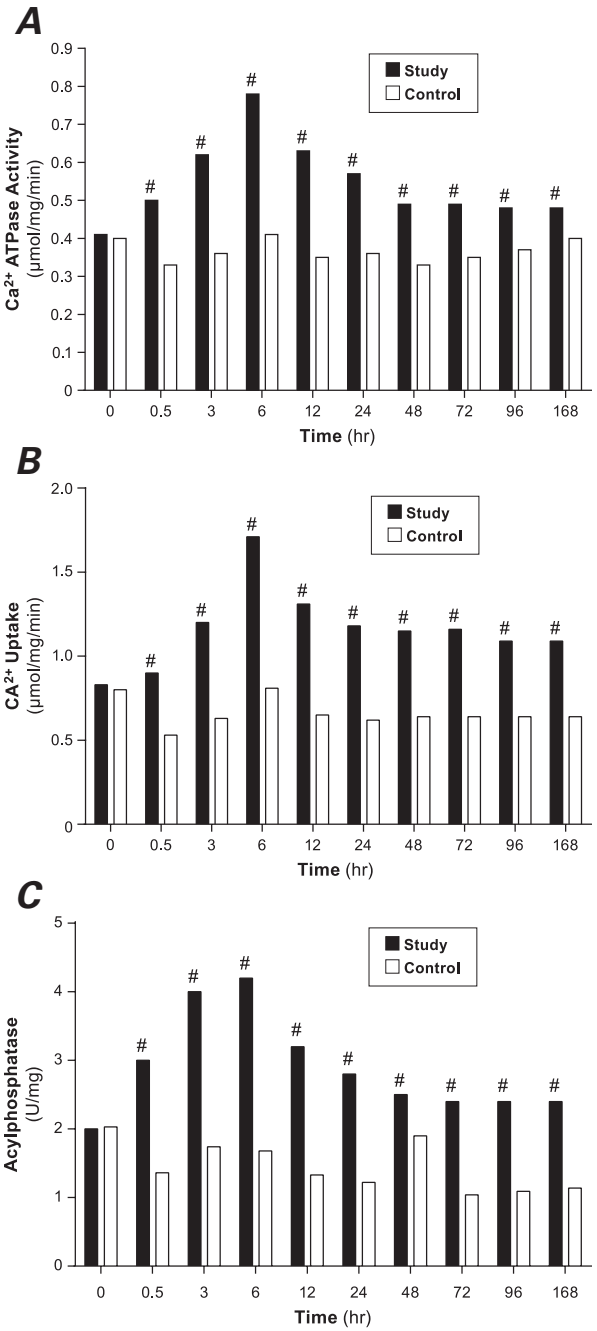

Fig. 4 *Time course of **A**) sarcoplasmic reticulum Ca^{2+}-ATPase activity, **B**) CA^{2+} uptake, and **C**) acylphosphatase in cardiac hypertrophy induced by pressure overload (black bars) and in sham-operated (control-group) pigs (white bars).*

#P <0.001 versus control values

Biochemical–Hemodynamic Correlations

Ca^{2+}-ATPase activity and Ca^{2+} uptake strongly correlates to acylphosphatase activity (r=0.91, P <0.001 and r=0.95, P <0.001, respectively). Table II shows correlations between indices of cardiac function and biochemical and morphologic changes at 6 hours of acute pressure overload.

A strong inverse correlation was found between PLB on the one hand and Ca^{2+}-ATPase activity, Ca^{2+}- uptake, SERCA2a, and indices of systolic function on the other hand. These correlations were not observed when we plotted these indices versus PLB.

Sarcoplasmic reticulum Ca^{2+}-ATPase is vital to overall heart function. The SERCA2a pump promotes muscle relaxation by lowering the cytosolic Ca^{2+} concentration and provides, through active Ca^{2+} transport, Ca^{2+} needed for the next contraction.[3] Phospholamban is an endogen regulator of SERCA2a: in its dephosphorylated status, it binds to SERCA2a and inhibits its activity. Phosphorylation of PLB by cyclic-AMP-dependent or calmodulin-dependent protein kinases (protein kinase A or calmodulin-dependent protein kinase II) relieves this inhibition, resulting in increased SERCA2a activity and increased SR Ca^{2+} loading,[14] which in turn generates larger action potentials during systole.[15]

Discussion

Very little is known about the early changes that occur during pressure overload before the onset of LVH, but more information is available about the biochemical and morphologic changes that occur in developed LVH and LV dysfunction, even in large mammals.[16,17]

This experimental study first attempted to explore the correlation, during the initial phases of acute pressure overload, between hemodynamics and changes in SR function, Ca^{2+} handling, SERCA2a activity, and SERCA2a expression. For these purposes, we subjected 54 farm pigs to acute pressure overload by encircling the ascending aorta; 18 sham-operated pigs formed our control group.

Pressure overload induced rapid changes in LV function. At 0.5 hr, the LV was the first to compensate—maintaining LVEF and stroke volume at the expense of higher end-diastolic volume. Heart rate significantly increased at 3 hr, thus maintaining cardiac output despite a significant reduction in systolic indices. At 6 hr, overload led to an evident state of myocardial dysfunction, with significant increases in end-diastolic pressure and wall stresses. This was confirmed by stress-short-

ening relations that, at 6 hr, showed that most pigs in the study group fell below the lower limit of normal function.

Left ventricular EDD and ESD rose immediately after banding and returned to baseline at 3 and 12 hr, respectively. We might suppose that EDD follows the trend of end-diastolic pressure, which (like EDD) rises at 3 and 6 hr, only to begin a steady reduction at 12 hr. Yet other factors (arterial stiffness, ventricular stiffness, and diastolic function), which have not been studied here, can better explain these similarities.

We found an increase in Ca^{2+} uptake and Ca^{2+}-ATPase activity, which reached its peak at 6 hr. This revealed a rapid increase in the calcium-transport capacity of SR, which progressively declined, still not reaching its baseline value after 96 hr. It has been shown that the expression levels of SERCA2a and Ca^{2+} transport decrease in pressure-overload-induced hypertrophy and heart failure[18,19] and that defective SR Ca^{2+} loading contributes to the onset of contractile failure in animals with chronic pressure overload.[20] The enhancement in Ca^{2+} fluxes between sarcoplasm and SR shown in this study might for the first time reveal the role that Ca^{2+} homeostasis plays as a compensatory mechanism for mechanical stress; this is perhaps confirmed by the strongly negative correlations that we found between Ca^{2+} uptake, Ca^{2+}-ATPase activity, and LV function values.

Another interesting thing to consider is that the increase in SERCA2a expression was lower than its activity, so it is possible that an independent SERCA2a-activating mechanism is at work here. We found acylphosphatase activity and its expression to increase substantially after pressure overload. Moreover, a strong correlation was found between changes in acylphosphatase activity after pressure overload and changes in Ca^{2+} uptake and Ca^{2+}-ATPase activity after pressure overload. Therefore, our results confirm a direct in-

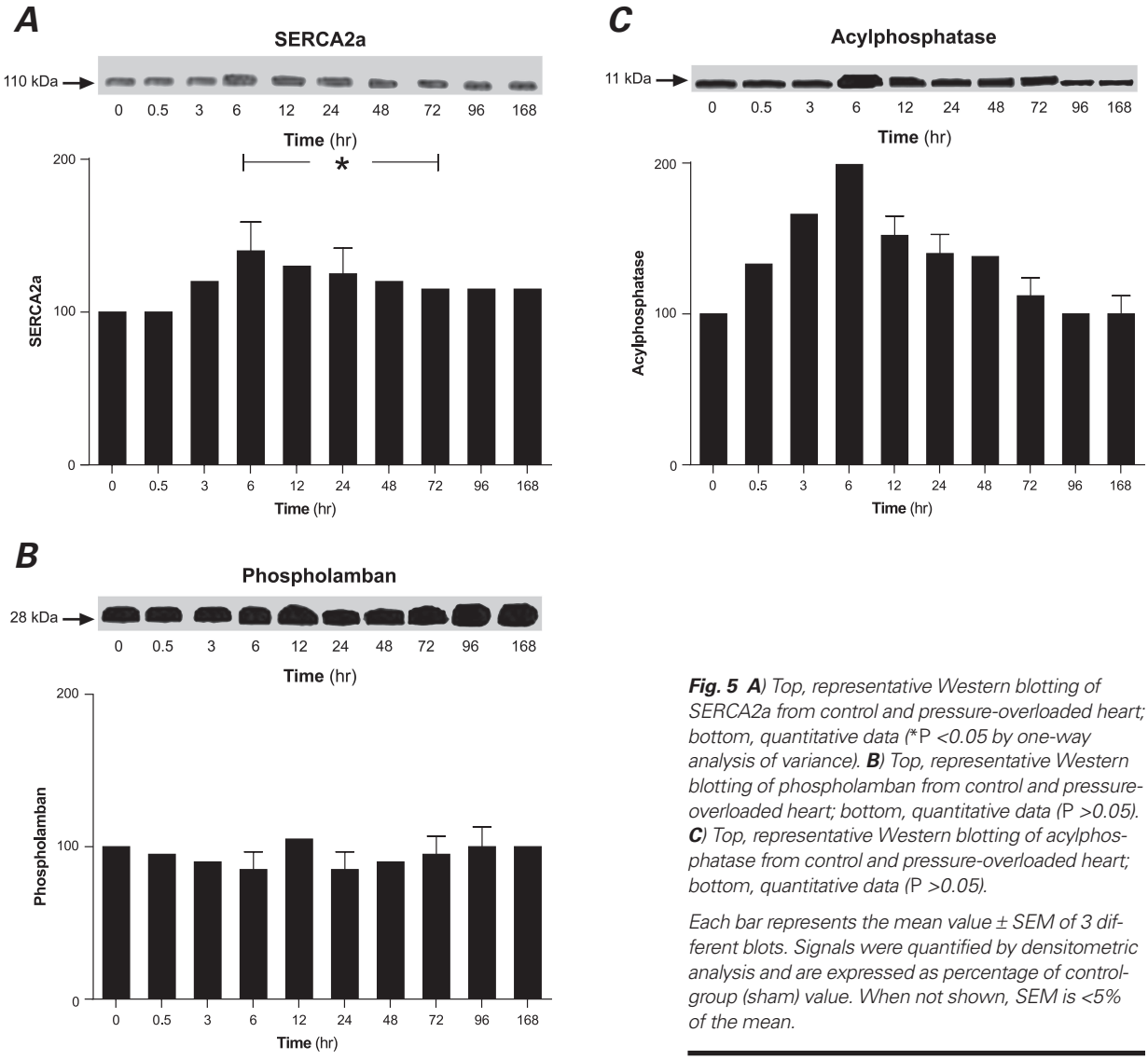

Fig. 5 ***A****) Top, representative Western blotting of SERCA2a from control and pressure-overloaded heart; bottom, quantitative data (*P <0.05 by one-way analysis of variance).* ***B****) Top, representative Western blotting of phospholamban from control and pressure-overloaded heart; bottom, quantitative data (*P >0.05). ***C****) Top, representative Western blotting of acylphosphatase from control and pressure-overloaded heart; bottom, quantitative data (*P >0.05).*

Each bar represents the mean value ± SEM of 3 different blots. Signals were quantified by densitometric analysis and are expressed as percentage of control-group (sham) value. When not shown, SEM is <5% of the mean.

volvement of acylphosphatase in the rise of Ca^{2+} pump activity and could explain the greater extent of Ca^{2+} uptake and ATP hydrolysis than would be expected from the relief of SERCA2a expression.

Our research group[21] showed that acylphosphatase induces increased activity of SERCA2a system by hydrolyzing the phosphoenzyme intermediate. In more recent studies,[22,23] we found further regulation of SERCA2a activity by acylphosphatase, through a physical displacement of the unphosphorylated PLB—an effect that was absent when the acylphosphatase structure was altered by thermal denaturation.[23,24] In these regards, it has been postulated that the action of acylphosphatase can be related to its conformational properties and particularly to its fragment that resembles the PLB cytoplasmic 1A domain, which is essential for the association of PLB with SERCA2a. This relationship with acylphosphatase-PLB was further confirmed by the fact that in skeletal muscle—where muscular SERCA2a is not associated with PLB—the regulation results in a so-called "uncoupling" effect with concomitant inhibition of Ca^{2+} transport. This effect is observed in other Ca^{2+} pumps lacking PLB, such as red-cell membrane and heart sarcolemmal Ca^{2+}-ATPase.[16,17] However, we failed to find in this study any significant change in PLB, either in its physiologic content or in its phosphorylated status. An interesting finding of our study was the significant increment in nuclear proto-oncogene c-fos expression detected by immunofluorescence, only at the 6-hr observation. This could support the hypothesis of involvement of this proto-oncogene in acute myocardial adaptation and in supporting cardiac contractility in early pressure overload through the synthesis of growing factors in response to a higher metabolic demand.[24] However, this finding needs confirmation; ad hoc investigations are in progress.

Finally, at morphologic analysis we found some focal derangement, along with rarefaction of contractile myofilaments, loss of sarcomeres, and intermyofibrillar edema. These findings might be related to Ca^{2+} handling. In fact, it has been shown that, in the presence of Ca^{2+} excess, some calcium-activated factors remove disks from myofibrils, thus contributing to metabolic turnover of myofibrillar proteins.[25]

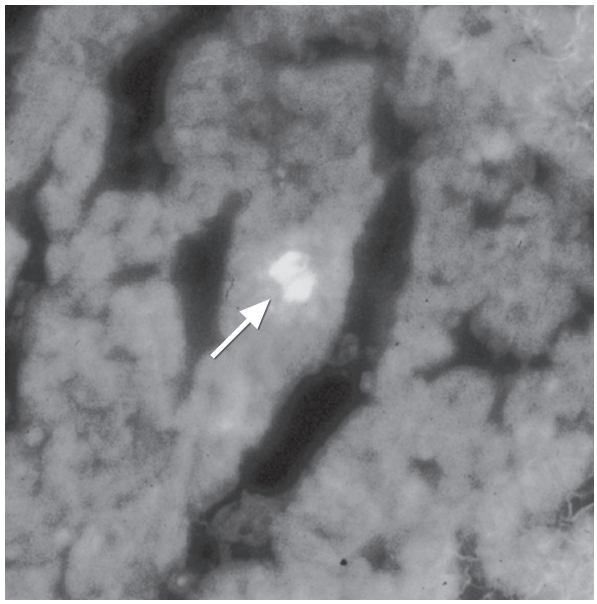

Fig. 6 *Immunofluorescence analysis with antibody anti-c-fos at 6-hr pressure overload. A substantial increase in nuclear proto-oncogene c-fos expression was detected (arrow).*

TABLE II. Biochemical–Hemodynamic Correlations

	Ca^{2+}-ATPase Activity		Ca^{2+} Uptake		SERCA2a Protein Level		Acylphosphatase Activity		Phospholamban	
Variable	***r***	***P* Value**	***r***	***P* Value**	***r***	***P* Value**	***r***	***P* Value**	***r***	***P* Value**
LVEF	−0.9012	<0.001	−0.8921	<0.001	−0.8413	<0.001	−0.8602	<0.001	0.2126	NS
FS_{endo}	−0.9133	<0.001	−0.9137	<0.001	−0.9032	<0.001	−0.8936	<0.001	0.2363	NS
FS_{mw}	−0.9712	<0.001	−0.9631	<0.001	−0.8831	<0.001	−0.9244	<0.001	0.2209	NS
CO	−0.9457	<0.001	−0.9361	<0.001	−0.8733	<0.001	−0.9057	<0.001	0.2041	NS
CI	−0.9236	<0.001	−0.9010	<0.001	−0.8131	<0.001	−0.8736	<0.001	0.2139	NS
SV	−0.9722	<0.001	−0.9553	<0.001	−0.8501	<0.001	−0.9021	<0.001	0.2236	NS
ESS_c	−0.9561	<0.001	−0.9312	<0.001	−0.9063	<0.001	−0.9233	<0.001	0.2341	NS
ESS_m	−0.9314	<0.001	−0.9249	<0.001	−0.8903	<0.001	−0.9015	<0.001	0.2301	NS

CI = cardiac index; CO = cardiac output; ESS_c = circumferential end-systolic stress; ESS_m = meridional end-systolic stress; FS_{endo} = endocardial fractional shortening; FS_{mw} = mid-wall fractional shortening; LVEF = left ventricular ejection fraction; NS = not significant; SERCA2a = sarcoplasmic reticulum Ca^{2+}-ATPase; SV = stroke volume

P <0.05 was considered statistically significant.

Limitations

The present study has certain limitations that need to be taken into account when evaluating results. First of all, most of the biochemical markers that we looked at were increased only for a brief period shortly after surgery, yet chronic changes in some values must have taken place to enable the progression of hemodynamic and echocardiographic measurements. In contrast, we did not report results from animals farther along in disease progression, in order to show how the model progresses. Furthermore, we did not look at the expression levels of additional transcription factors and mediators, such as GATA4, MEF2, and ATF3, which play an important role during pressure overload and cardiac hypertrophy. The function of these factors and their correlation with LV function and Ca metabolism warrant further investigation.

Conclusions

In our model of induced pressure overload, an initial phase of depressed myocardial contractility was accompanied by enhanced SR function and higher Ca^{2+}-ATPase and Ca^{2+} uptake activities, mediated by acylphosphatase. This new finding of Ca^{2+} homeostasis might indicate a compensatory mechanism for mechanical stress. Further studies need to confirm our findings and to evaluate the role of all these factors in the early myocardial response to acute pressure overload.

References

1. Frohlich ED, Apstein C, Chobanian AV, Devereux RB, Dustan HP, Dzau V, et al. The heart in hypertension [published erratum appears in N Engl J Med 1992;327(24):1768]. N Engl J Med 1992;327(14):998-1008.
2. Aurigemma GP, Silver KH, McLaughlin M, Mauser J, Gaasch WH. Impact of chamber geometry and gender on left ventricular systolic function in patients > 60 years of age with aortic stenosis. Am J Cardiol 1994;74(8):794-8.
3. Bers DM. Cardiac excitation-contraction coupling. Nature 2002;415(6868):198-205.
4. Levitsky D, de la Bastie D, Schwartz K, Lompre AM. Ca(2+)-ATPase and function of sarcoplasmic reticulum during cardiac hypertrophy. Am J Physiol 1991;261(4 Suppl):23-6.
5. Nediani C, Formigli L, Perna AM, Ibba-Manneschi L, Zecchi-Orlandini S, Fiorillo C, et al. Early changes induced in the left ventricle by pressure overload. An experimental study on swine heart. J Mol Cell Cardiol 2000;32(1):131-42.
6. Sahn DJ, DeMaria A, Kisslo J, Weyman A. Recommendations regarding quantitation in M-mode echocardiography: results of a survey of echocardiographic measurements. Circulation 1978;58(6):1072-83.
7. Devereux RB, Reichek N. Echocardiographic determination of left ventricular mass in man. Anatomic validation of the method. Circulation 1977;55(4):613-8.
8. Aurigemma GP, Gaasch WH. Quantitative evaluation of left ventricular structure, wall stress and systolic function. In: Otto CM, editor. The practice of clinical echocardiography. 4th ed. Philadelphia: Elsevier/Saunders; 2012. p. 156-76.
9. Shimizu G, Zile MR, Blaustein AS, Gaasch WH. Left ventricular chamber filling and midwall fiber lengthening in patients with left ventricular hypertrophy: overestimation of fiber velocities by conventional midwall measurements. Circulation 1985;71(2):266-72.
10. Wyatt HL, Heng MK, Meerbaum S, Gueret P, Hestenes J, Dula E, Corday E. Cross-sectional echocardiography. II. Analysis of mathematic models for quantifying volume of the formalin-fixed left ventricle. Circulation 1980;61(6):1119-25.
11. de Simone G, Devereux RB, Roman MJ, Ganau A, Saba PS, Alderman MH, Laragh JH. Assessment of left ventricular function by the midwall fractional shortening/end-systolic stress relation in human hypertension [published erratum appears in J Am Coll Cardiol 1994;24(3):844]. J Am Coll Cardiol 1994;23(6):1444-51.
12. Grossman W, Jones D, McLaurin LP. Wall stress and patterns of hypertrophy in the human left ventricle. J Clin Invest 1975;56(1):56-64.
13. Gasser JT, Chiesi MP, Carafoli E. Concerted phosphorylation of the 26-kilodalton phospholamban oligomer and of the low molecular weight phospholamban subunits [published erratum appears in Biochemistry 1987;26(8):2400]. Biochemistry 1986;25(23):7615-23.
14. MacLennan DH, Kranias EG. Phospholamban: a crucial regulator of cardiac contractility. Nat Rev Mol Cell Biol 2003;4(7):566-77.
15. Braz JC, Gregory K, Pathak A, Zhao W, Sahin B, Klevitsky R, et al. PKC-alpha regulates cardiac contractility and propensity toward heart failure. Nat Med 2004;10(3):248-54.
16. Aoyagi T, Fujii AM, Flanagan MF, Arnold L, Mirsky I, Izumo S. Maturation-dependent differences in regulation of sarcoplasmic reticulum Ca(2+) ATPase in sheep myocardium in response to pressure overload: a possible mechanism for maturation-dependent systolic and diastolic dysfunction. Pediatr Res 2001;50(2):246-53.
17. Hirsch JC, Borton AR, Albayya FP, Russell MW, Ohye RG, Metzger JM. Comparative analysis of parvalbumin and SERCA2a cardiac myocyte gene transfer in a large animal model of diastolic dysfunction. Am J Physiol Heart Circ Physiol 2004;286(6):H2314-21.
18. Matsui H, MacLennan DH, Alpert NR, Periasamy M. Sarcoplasmic reticulum gene expression in pressure overload-induced cardiac hypertrophy in rabbit. Am J Physiol 1995;268(1 Pt 1):C252-8.
19. Qi M, Shannon TR, Euler DE, Bers DM, Samarel AM. Downregulation of sarcoplasmic reticulum Ca(2+)-ATPase during progression of left ventricular hypertrophy. Am J Physiol 1997;272(5 Pt 2):H2416-24.
20. Kiss E, Ball NA, Kranias EG, Walsh RA. Differential changes in cardiac phospholamban and sarcoplasmic reticular Ca(2+)-ATPase protein levels. Effects on Ca2+ transport and mechanics in compensated pressure-overload hypertrophy and congestive heart failure. Circ Res 1995;77(4):759-64.
21. Nediani C, Fiorillo C, Marchetti E, Pacini A, Liguri G, Nassi P. Stimulation of cardiac sarcoplasmic reticulum calcium pump by acylphosphatase. Relationship to phospholamban phosphorylation. J Biol Chem 1996;271(32):19066-73.
22. Nediani C, Fiorillo C, Rigacci S, Magherini F, Francalanci M, Liguri G, et al. A novel interaction mechanism accounting for different acylphosphatase effects on cardiac and fast twitch skeletal muscle sarcoplasmic reticulum calcium pumps. FEBS Lett 1999;443(3):308-12.
23. Nediani C, Celli A, Formigli L, Perna AM, Fiorillo C, Ponziani V, et al. Possible role of acylphosphatase, Bcl-2 and Fas/Fas-L system in the early changes of cardiac remodeling induced by volume overload. Biochim Biophys Acta 2003;1638(3):217-26.

24. Modesti PA, Vanni S, Bertolozzi I, Cecioni I, Polidori G, Paniccia R, et al. Early sequence of cardiac adaptations and growth factor formation in pressure- and volume-overload hypertrophy. Am J Physiol Heart Circ Physiol 2000;279(3):H976-85.

25. Badalamente MA, Hurst LC, Stracher A. Localization and inhibition of calcium-activated neutral protease (CANP) in primate skeletal muscle and peripheral nerve. Exp Neurol 1987;98(2):357-69.

Appendix. Biochemical and Morphologic Evaluation

Preparation of Sarcoplasmic Reticulum Vesicles

After excision, each heart was cut with scissors and rinsed in ice-cold 0.9% sodium chloride solution to remove all traces of blood. Specimens were homogenized 4 times with an ULTRA-TURRAX® apparatus (IKA® Works, Inc.; Wilmington, NC) in 4 volumes of 10-mM sodium bicarbonate (pH, 7), containing 1 mM phenylmethylsulfonyl fluoride (PMSF), 10 µg/mL leupeptin and aprotinin, for 10 s. Homogenates were centrifuged at 5,000 × g for 10 min. The supernatants were filtered through a 4-layer cheesecloth before centrifugation at 12,000 × g for 15 min. The supernatants were filtered again and centrifuged at 100,000 × g for 30 min. The pellets were resuspended in potassium chloride (KCl) (0.6 M) and histidine (30 Mm), then centrifuged at 100,000 × g. The final pellets, corresponding to microsomal fractions rich in sarcoplasmic reticulum (SR) vesicles, were suspended in sucrose (0.3 M) and histidine (30 Mm), both pH 7.

ATPase Activity Measurements

SERCA2a total activity was assayed in a standard reaction mixture containing 50 M Tris(hydroxymethyl) aminomethane hydrochloride (Tris-HCl), 3 mM magnesium chloride, 100 mM KCl, 5 mM sodium azide, 50 µM calcium chloride ($CaCl_2$), 3 mM adenosine-5′-triphosphate, 1 Mm ouabain, and 50 µg/mL vesicle protein. Ouabain and sodium azide were added in order to inhibit sarcolemmal Na^+. K^+-ATPase and mitochondrial ATPase, respectively, eventually present as contaminants in SR vesicles preparations. In these conditions, a free Ca^{2+} concentration of approximately 10 µM was calculated by using the equations of Katz. To determine basal ATPase activity, the assays were carried out in the presence of 1 mM ethylene glycol tetraacetic acid (Tris-EGTA) instead of $CaCl_2$. Reactions were started by the addition of ATP and stopped after 10 min with 1 volume of ice-cold 20% trichloroacetic acid. After centrifugation (12,000 × g for 5 min), the amount of released inorganic phosphate (Pi) was measured by means of the malachite-green staining procedure. Ca^{2+}-dependent ATPase activity was estimated by subtracting the basal ATPase activity from the total Ca^{2+}-ATPase.

Ca^{2+} Uptake Measurements

Ca^{2+} influx measurements into SR vesicles were carried out using the same reaction mixture as is used for ATPase assays, except that this measure included $^{45}CaCl_2$ and 5 mM oxalate. After 30 s of incubation at 37 °C, vesicles were separated by filtration through a Millipore filter (pore size, 0.45 µm), immediately washed twice with 4 mL of ice-cold 20-mM Tris-HCl (pH 7.4), 1 mM ethylene glycol tetraacetic acid, and 100 mM KCl. ^{45}Ca uptake was measured as the difference in ^{45}Ca influx into the vesicle at zero time and at the end of incubation. Radioactivity trapped on the filter was determined by liquid scintillation spectroscopy.

Acylphosphatase Activity Measurements

To measure acylphosphatase activity, cardiac ventricles were homogenized with 4 volumes of 0.1 molar (M) hydrochloric acid and centrifuged at 15,000 × g for 20 min. Supernatants were collected, adjusted to pH 5.3 (the optimal pH of this enzyme), and centrifuged at 15,000 × 9 for 20 min. Supernatants of this centrifugation were collected for protein and activity determination. Acylphosphatase activity was performed by a continuous optical test at 283 nm, using benzoyl phosphate as substrate.

Western Blot Analysis of SERCA2a, Phospholamban, and Acylphosphatase

To analyze SERCA2a, phospholamban and acylphosphatase specimens were homogenized 3 times at half the maximal speed with an ULTRA-TURRAX apparatus in 4 volumes of 10 mM sodium bicarbonate solution containing 1 mM PMSF, 10 µg/mL leupeptin and aprotinin, for 15 s. Three hundred µL of each homogenate was added to 600 µL of 20% sodium dodecyl sulfate. Mixtures were incubated at 25 °C for 20 min before centrifugation for 30 min at 100,000 × g. Supernatants were collected and assayed for protein concentration by the biuret method. Equal amounts of proteins (30 µg) were separated on 8% or on high-resolution 15% sodium dodecyl sulfate polyacrylamide gel electrophoresis (SDS-PAGE) gels. To improve resolution, the 15% gels were left at room temperature for at least 24 hr to obtain complete polymerization and were then run at lower current (20 mA instead of routine 30 mA). Then gels were electroblotted to nitrocellulose membranes, and nonspecific binding sites were blocked for 2 hr in 5% phosphate buffered saline – tris buffered saline with Tween-20 (PBS–TBST) solution (50 mM Tris-HCl [pH, 7.4], 150 mM sodium chloride, 0.1% Tween 20), with agitation. Membranes from

8% gel were incubated with 1:500 diluted monoclonal (mouse) anti-SERCA2a-ATPase-antibody. In contrast, proteins transferred from the 15% gel were incubated overnight with 0.2 µg/mL polyclonal (rabbit) anti-human muscle acylphosphatase antibody (elevated in rabbits using recombinant protein and purified by affinity chromatography) or 2 µg/mL monoclonal (mouse) anti-phospholamban antibody at 4 °C. Immunodetections of the primary antibody against SERCA2a and phospholamban were carried out with a 1:10,000 diluted peroxidase-conjugated anti-mouse immunoglobulin G secondary antibody; for acylphosphatase, immunodetections were carried out with 1:20,000 diluted peroxidase-conjugated anti-rabbit immunoglobulin G secondary antibody (dilution buffer: 50 mM Tris-HCL [pH 7.4], 150 mM sodium chloride, and 0.1% Tween 20) for 1 hr at room temperature. Blots were then incubated with ECL™ detection reagent (GE Healthcare; Wausheka, Wisc) for 1 min and exposed to Kodak® BioMax® Light Autoradiography film. Signals were quantified using the QuantiScan program (Biosoft; Cambridge, UK) for image analysis and densitometry. The mean signal value in the sham-operated pigs was defined as 100% and the signal density for each overloaded heart was calculated as a percentage of the mean value obtained from the control pigs within the same blot.

Morphologic Analysis

For the ultrastructural analysis, myocardial biopsies were taken from the left ventricular wall of each animal, immediately fixed by immersion in cold 2.5% glutaraldehyde in 0.1 M cacodylate buffer (pH, 7.4) at room temperature, and postfixed in 1% osmium tetroxide in 0.1 M phosphate buffer (pH, 7.4) at room temperature. Specimens were then dehydrated in a graded acetone series, passed through propylene oxide, and embedded in Epon 812 resin. Semi-thin sections (2 µm) were cut, stained with toluidine blue-sodium tetraborate, and observed under a light microscope. Ultrathin sections were placed on a 200-mesh copper grid, stained with uranyl acetate and alkaline bismuth subnitrate, and then examined under a transmission electron microscope.